Hirschey *et al*, Supplementary Figure 1

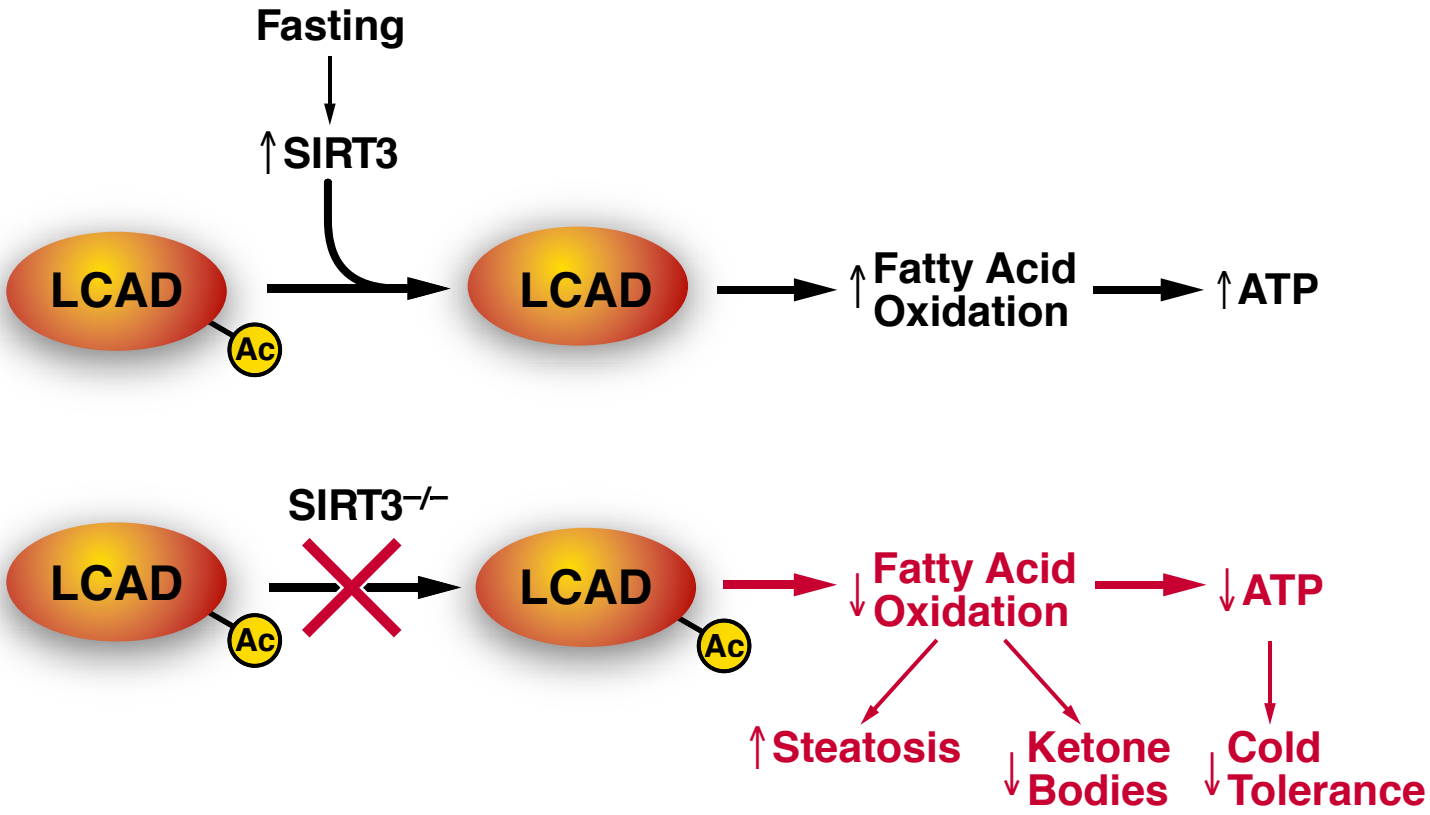

Hirschey *et al*, Supplementary Figure 2

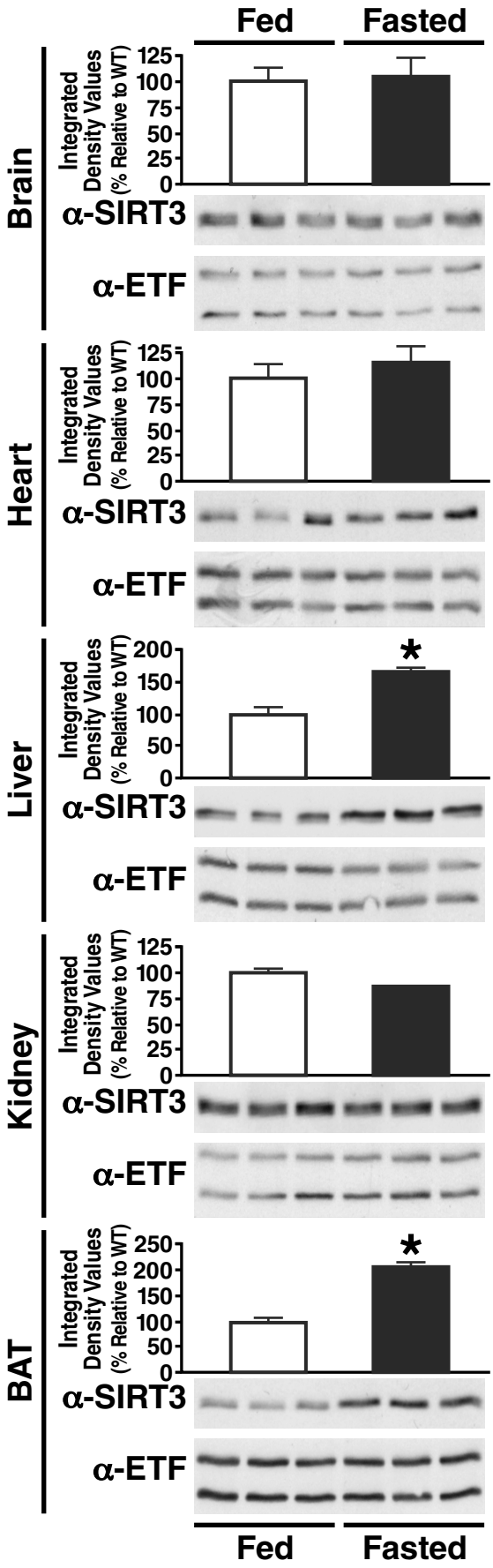

Hirschey *et al*, Supplementary Figure 3

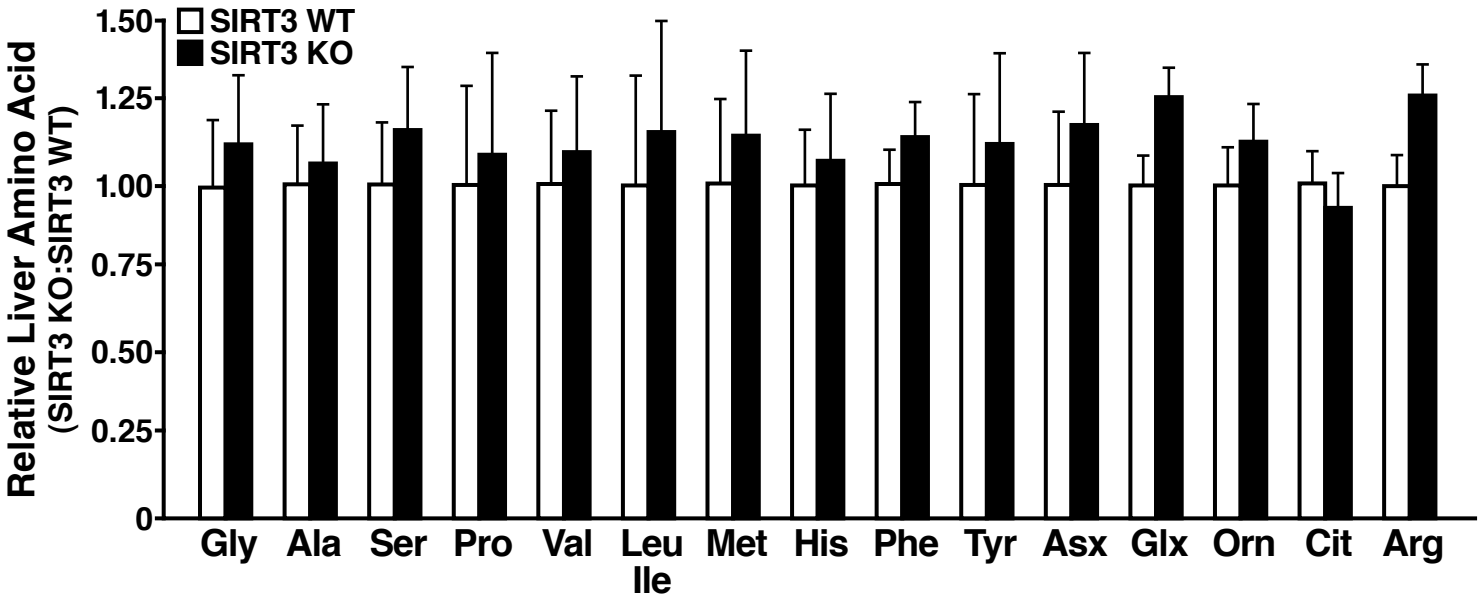

Hirschey *et al*, Supplementary Figure 4

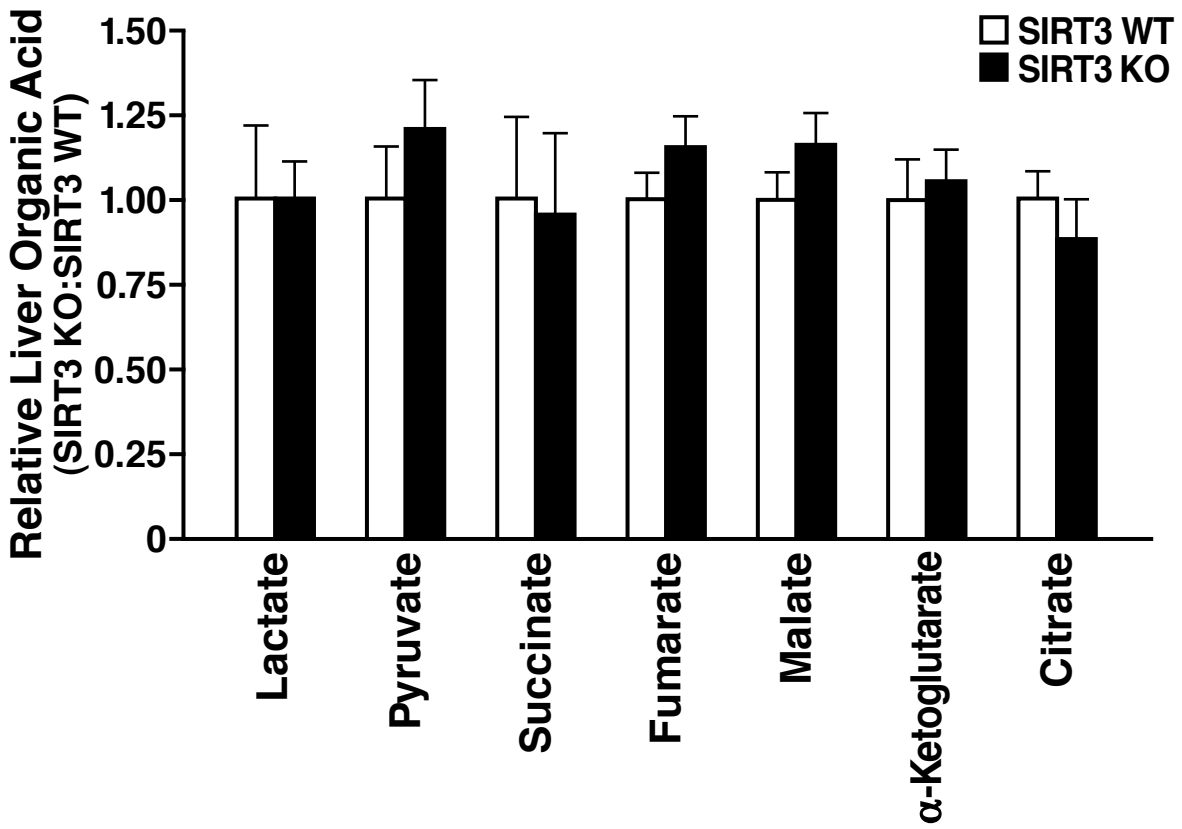

Hirschey *et al*, Supplementary Figure 5

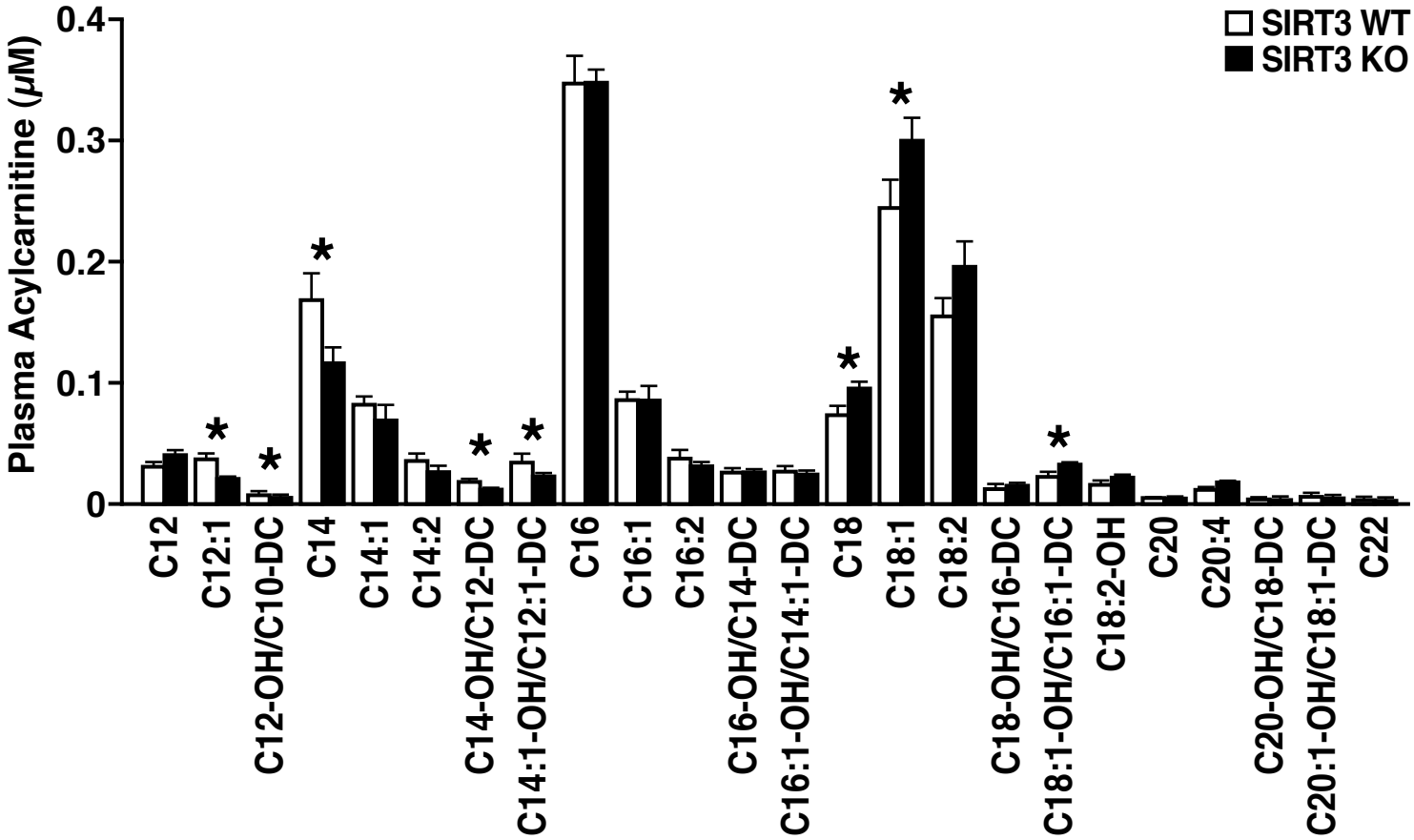

Hirschey *et al*, Supplementary Figure 6

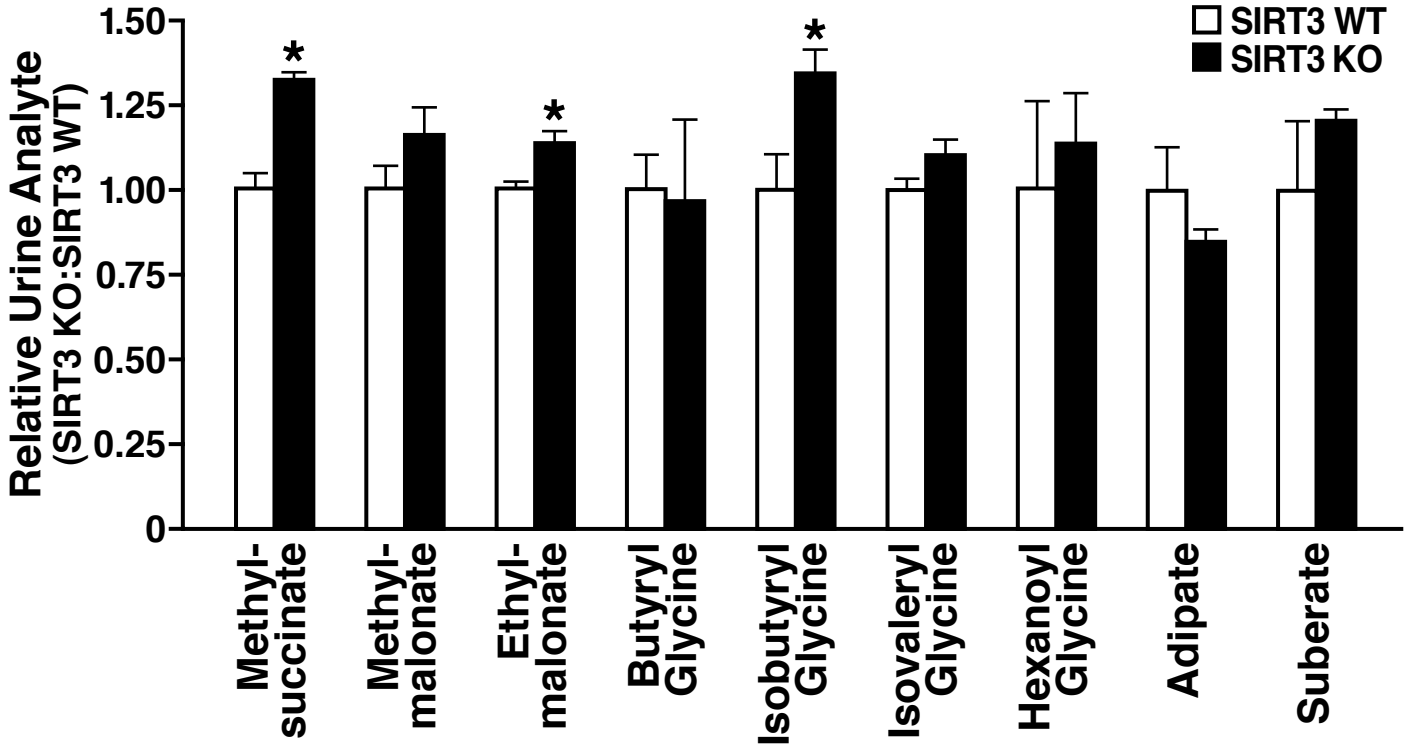

Hirschey *et al*, Supplementary Figure 7

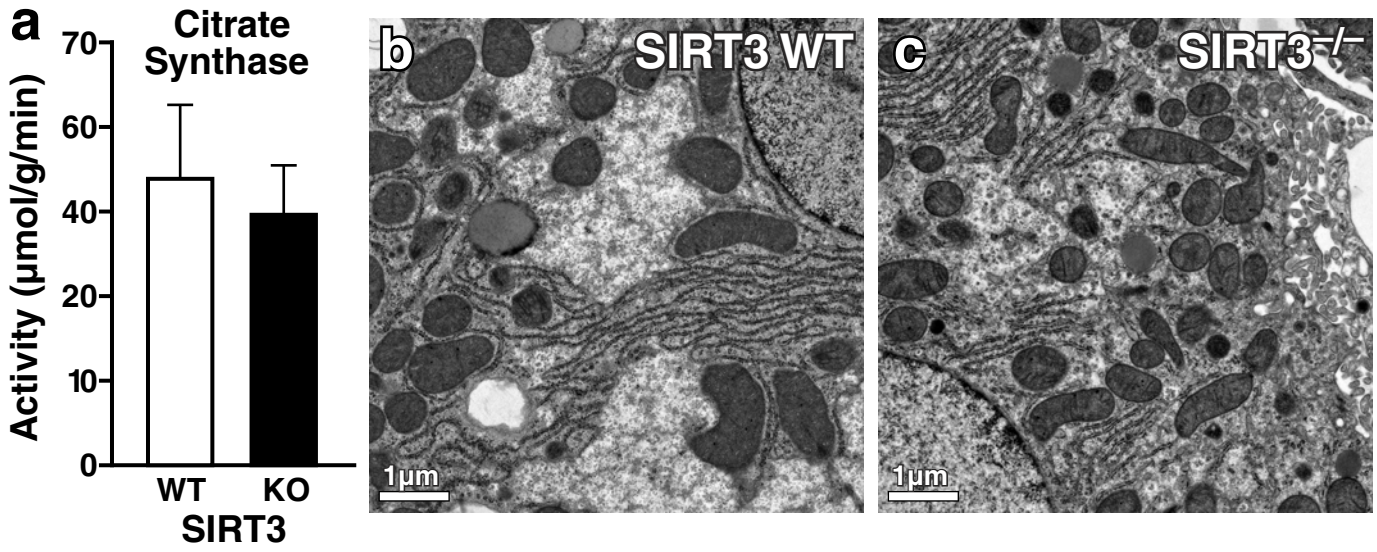

Hirschey *et al*, Supplementary Figure 8

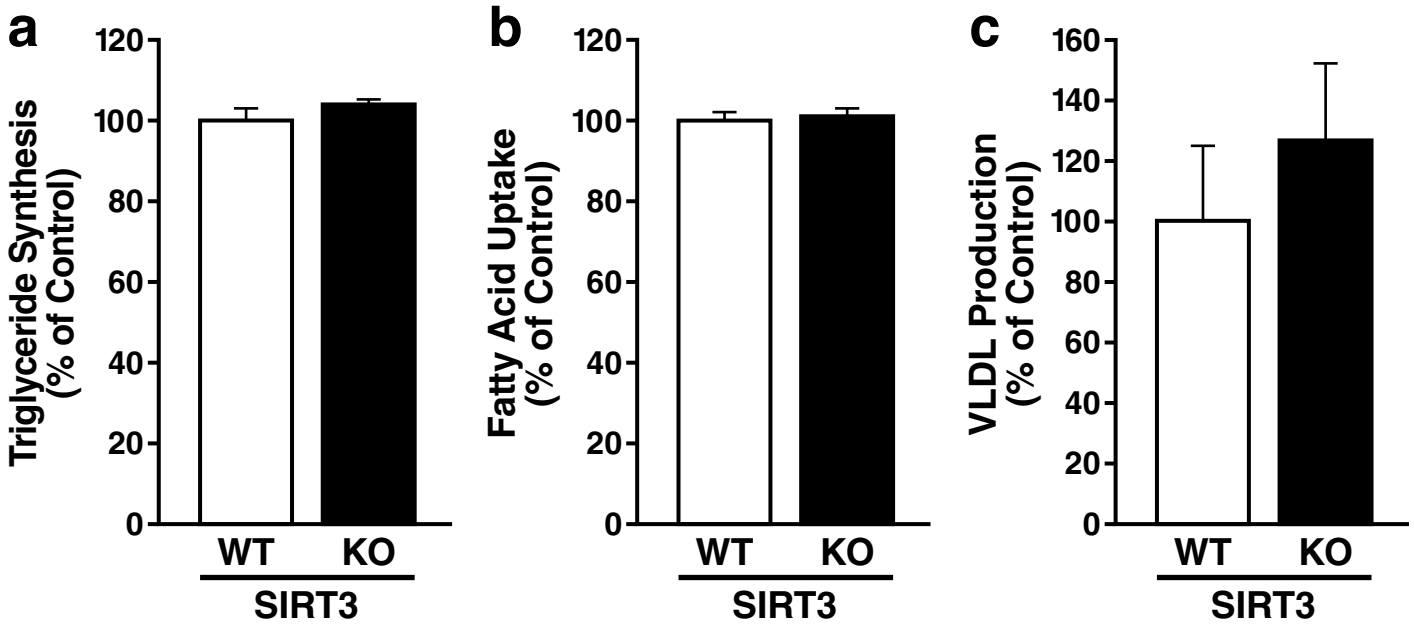

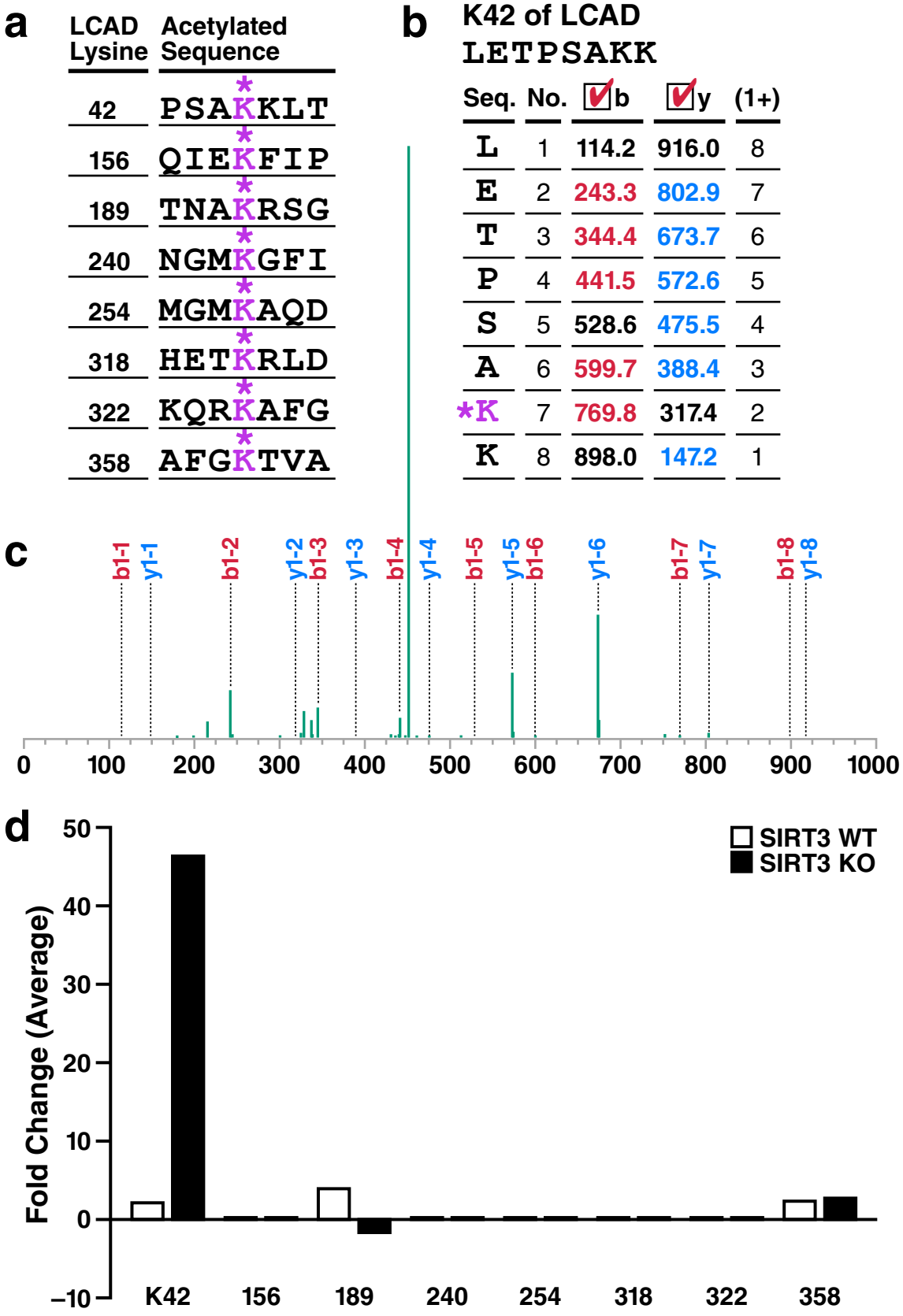
a
LCAD Lysine
Acetylated Sequence
42 PSAK*KLT
156 QIEK*FIP
189 TNAK*RSG
240 NGMK*GFI
254 MGMK*AQD
318 HETK*RLD
322 KQRK*AFG
358 AFGK*TVA
b
K42 of LCAD
LETPSAKK
Seq. No. b y (1+)
L 1 114.2 916.0 8
E 2 243.3 802.9 7
T 3 344.4 673.7 6
P 4 441.5 572.6 5
S 5 528.6 475.5 4
A 6 599.7 388.4 3
*K 7 769.8 317.4 2
K 8 898.0 147.2 1
c
b1-1 y1-1 b1-2 y1-2 b1-3 y1-3 b1-4 y1-4 b1-5 y1-5 b1-6 y1-6 b1-7 y1-7 b1-8 y1-8
0 100 200 300 400 500 600 700 800 900 1000
d
SIRT3 WT
SIRT3 KO
Fold Change (Average)
50 40 30 20 10 0 −10
K42 156 189 240 254 318 322 358

A

```
hLCAD   MAARLL-RGSLRVLGGHRAPRQLPAARCSHSGGEERLETPSAKKLTDIGIRRIFSPEHDI  59
        ****** * *****    ***  *+******* * ***********+******* ****
mLCAD   MAARLLLR-SLRVLKARSAPRPPPSARCSHSGAEARLETPSAKKLTDVGIRRIFSSEHDI  59

hLCAD   FRKSVRKFFQEEVIPHHSEWEKAGEVSREVWEKAGKQGLLGVNIAE-HLGGIGGDLYSAA  118
        **+**************+*************************+**** * ******* * *
mLCAD   FRESVRKFFQEEVIPHHTEWEKAGEVSREVWEKAGKQGLLGINIAEKH-GGIGGDLLSTA  118

hLCAD   IVWEEQAYSNCSGPGFSIHSGIVMSYITNHGSEEQIKHFIPQMTAGKCIGAIAMTEPGAG  178
        + *********+******+** *** ** *+++++***+ **********************
mLCAD   VTWEEQAYSNCTGPGFSLHSDIVMPYIANYGTKEQIEKFIPQMTAGKCIGAIAMTEPGAG  178

hLCAD   SDLQGIKTNAKKDGSDWILNGSKVFISNGSLSDVVIVVAVTNHEAPSPAHGISLFLVENG  238
        *****+*****+ ***************** ***+********* ** **************
mLCAD   SDLQGVRTNAKRSGSDWILNGSKVFITNGWLSDLVIVVAVTNREARSPAHGISLFLVENG  238

hLCAD   MKGFIKGRKLHKMGLKAQDTAELFFEDIRLPASALLGEENKGFYYIMKELPQERLLIADV  298
        **************+************+****+************+*+***********++
mLCAD   MKGFIKGRKLHKMGMKAQDTAELFFEDVRLPANALLGEENKGFYYLMQELPQERLLIAEL  298

hLCAD   AISASEFMFEETRNYVKQRKAFGKTVAHLQTVQHKLAELKTHICVTRAFVDNCLQLHEAK  358
        **** ************************+**********************+****** *
mLCAD   AISACEFMFEETRNYVKQRKAFGKTVAHIQTVQHKLAELKTHICVTRAFVDSCLQLHETK  358

hLCAD   RLDSATACMAKYWASELQNSVAYDCVQLHGGWGYMWEYPIAKAYVDARVQPIYGGTNEIM  418
        **** +* ***************+************************************
mLCAD   RLDSGSASMAKYWASELQNSVAYECVQLHGGWGYMWEYPIAKAYVDARVQPIYGGTNEIM  418

hLCAD   KELIAREIVFD  429
        ********* *
mLCAD   KELIARQIVSD  429
```

B

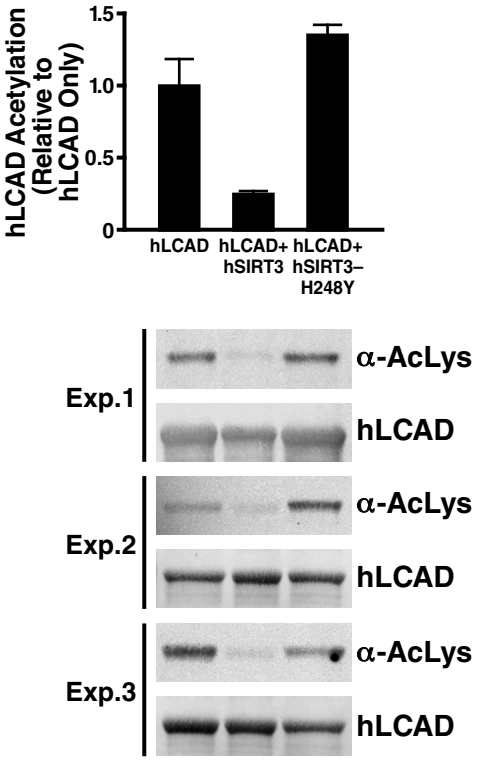

C

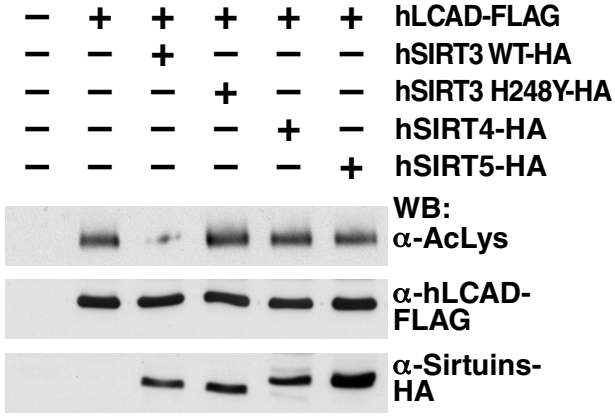

Hirschey *et al*, Supplementary Table 1

	Fed		Fasted	
SIRT3:	**WT**	**KO**	**WT**	**KO**
Glucose (mg/dL)	**297**	**264**	**102**	**103**
Free Fatty Acid (mM)	**0.37**	**0.32**	**1.23**	**1.14**
Ketone Bodies (mM)	**0.21**	**0.18**	**1.58**	**1.32***

Supplementary Figure Legends

Figure S1. Working model. The increase in SIRT3 protein during fasting decreases the acetylation of LCAD, an important fatty acid oxidation (FAO) enzyme, resulting in increased FAO flux and energy production. In SIRT3-/-mice, LCAD remains hyperacetylated, resulting in reduced FAO that causes steatosis, reduced ketone body production, and reduced ATP generation resulting in cold intolerance.

Figure S2. Fasting induces SIRT3 expression in oxidative tissues.
Mitochondria isolated from tissues of fed or fasted (~24 h) wild-type mice were analyzed by western blotting analysis with an antiserum specific for SIRT3, electron transfer flavoprotein (ETF) was used as a reference, integrated density values were calculated for fed and fasted wild-type mice.

Figure S3. SIRT3-/- and wt mice show no differences in metabolomic profiling of hepatic amino acids.
Metabolomic analysis was conducted on mouse liver tissue, and data obtained in SIRT3-/- mice are shown relative to wt mice (n=5/genotype, fasted 24 h).

Figure S4. SIRT3-/- and wt mice show no differences in metabolomic profiling of hepatic organic acids.
Metabolomic analysis was conducted on mouse liver tissue, and data obtained in SIRT3-/- mice are shown relative to wt mice (n=5/genotype, fasted 24 h).

Figure S5. Abnormal accumulation of long-chain acylcarnitines in the livers of mice lacking SIRT3 during fasting.
Metabolomic analysis was conducted on mouse liver tissue, and data obtained in wt and SIRT3-/- mice are given in absolute values; data correspond to relative values in Figure 2b (n=5/genotype, fasted 24 h), $^{*}p<0.05$.

Figure S6. Abnormal excretion of urine analytes in mice lacking SIRT3 during

fasting.

Metabolomic analysis was conducted on mouse urine, and data obtained in SIRT3-/- mice are shown relative to wt mice (n=5/genotype, fasted 24 h), $^{*}p<0.05$.

Figure S7. SIRT3-/- and wt mice show no differences in hepatic citrate synthase activity, and electron micrographs are similar.

a. Citrate synthase enzyme activity was measured in mouse liver tissue *ex vivo* (n=10/genotype from two separate trials, fasted 24 h), p=NS; **b, c.** Transmission electron micrograph images from wt (panel b) and SIRT3-/- (panel c) liver tissue.

Figure S8. Rates of lipogenesis, lipid uptake and lipid export are similar in wt and SIRT3-/- mice.

a. Radiolabeled ^{14}C-oleic acid triglyceride synthesis was measured in wt and SIRT3-/- mouse primary hepatocytes (two independent hepatocyte preparations, n=5 measurements/sample). **b.** Radiolabeled ^{14}C-oleic acid lipid uptake was measured in wt and SIRT3-/- mouse primary hepatocytes (two independent hepatocyte preparations, n=5 measurements/sample). **c.** VLDL lipid export was measured in wt and SIRT3-/- mice (n=6/genotype, fasted 5 h), p=NS

Figure S9. Mass spectrometry analysis identified eight sites of LCAD acetylation, and LCAD lysine 42 is hyperacetylated in SIRT3-/- mice.

a. Summary peptide fragment table from acetylated lysine residues; **b, c.** Representative m/z spectra (K42) obtained from mass spectrometry analyses of LCAD from purified mouse liver mitochondria in wt and SIRT3-/- mice; **d.** Differential acetylation fold values for LCAD acetylated lysines from wt and SIRT3-/- hepatic mouse mitochondria.

Figure S10. SIRT3 deacetylates human LCAD *in vitro* and *in vivo*.

a. Protein sequence alignment between hLCAD (top) and mLCAD (bottom); **b.** Purified recombinant hLCAD expressed in *E. coli* was incubated *in vitro* with recombinant hSIRT3 or hSIRT3-H248Y (catalytically-inactive SIRT3 mutant); **c.** Expression vectors for wt hSIRT3, hSIRT3-H248Y (catalytically-inactive SIRT3 mutant), hSIRT4, or

hSIRT5 were co-transfected into HEK293 cells with expression vectors for FLAG-tagged hLCAD, and the level of acetylation of hLCAD was assessed after anti-FLAG immunoprecipitation followed by western blotting using an anti-acetyllysine antiserum.

Table S1. Metabolic parameters were measured and recorded in wt and SIRT3-/- mice under fed and fasted conditions.